ACS Sustainable Chemistry & Engineering

pubs.acs.org/journal/ascecg

Research Article

# Homogeneous Pd-Catalyzed Heck Coupling in γ-Valerolactone as a Green Reaction Medium: A Catalytic, Kinetic, and Computational Study

Dániel Fodor, Tamás Kégl, József M. Tukacs, Attila K. Horváth,* and László T. Mika*

Cite This: *ACS Sustainable Chem. Eng.* 2020, 8, 9926−9936

Read Online

ACCESS | Metrics & More | Article Recommendations | Supporting Information

**ABSTRACT:** γ-Valerolactone (GVL) was proposed as an environmentally benign reaction medium for phosphine-free Pd-catalyzed homogeneous Heck coupling reaction of iodobenzene and styrene derivatives. Detailed catalytic, kinetic, and computational studies were performed for this industrially important transformation in GVL, which shows remarkable tolerance for the moisture content of the reaction mixture and gives good efficiency for Pd(II) catalyst precursors such as $PdCl_2$ and $Pd(OAc)_2$. Excellent functional group tolerance for both iodoaromatic substances and styrene derivatives was shown, and the reaction efficiency was correlated by the Hammet-constant of corresponding substrates. A simplified kinetic model was subsequently found to model the transformation, which can be represented by an excellent fitting of the calculated concentration of corresponding species to the experimentally determined ones. $\Delta H^{\ddagger}_{app}$ = +103.0 kJ·mol$^{-1}$ for the apparent overall activation enthalpy of the reaction in GVL, and $\Delta H^{\ddagger}_{app}$ = +103.7 kJ·mol$^{-1}$ in the case of DMF have been obtained. $\Delta S^{\ddagger}_{app}$ = +139.7 J·mol$^{-1}$·K$^{-1}$ was calculated for the apparent overall activation entropy of the reaction in the presence of GVL, and $\Delta S^{\ddagger}_{app}$ = +138.1 J·mol$^{-1}$·K$^{-1}$ in the presence of DMF, very similar values suggesting that no medium effect on the mechanism can be proposed. The computational study confirmed the experimentally observed trends regarding the effect of electron-donating and -withdrawing substituents of iodobenzene and styrene as follows: the electron-donating substituents accelerate the reaction rate for iodobenzene but decrease the reactivity for styrene derivatives.

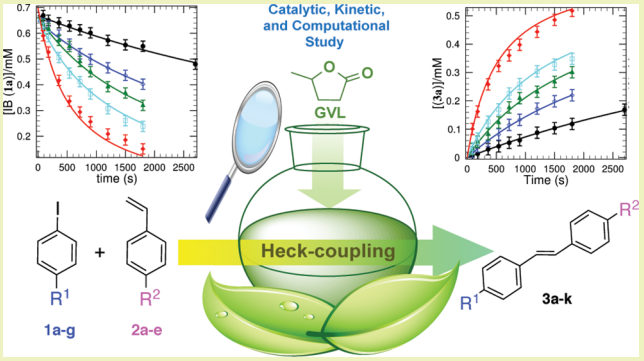


**KEYWORDS:** *γ-valerolactone, green solvent, Heck coupling, kinetic model, homogeneous catalysis*

## INTRODUCTION

The modern chemical industry that almost exclusively depends on fossil-based carbon resources provides millions of products that maintain or even increase the living standards of our society.[1] Within these technological systems, the properties of synthetic transformation(s), as the heart of the process, play a key role in the molecular level control of the environmental impact from chemical production. The elimination of hazardous substances and fossil-based auxiliary materials from synthesis schemes without any decrease in efficiency may establish alternatives toward corresponding green technologies.[2−5]

Oil refineries, having a throughput of almost 83 000 barrels per day,[6] continuously provide resources for the chemical industry from bulk chemicals and reagents to organic solvents, an estimated industrial-scale annual production of almost 20 million metric tons.[7] The solvent as an intrinsic part of the chemical reactions can have a significant influence on the outcome of both stoichiometric or even catalytic reactions. Therefore, the introduction and viable utilization of non-fossil-based reaction media in the chemical industry are one of the most crucial challenges in the development of cleaner production of consumer products.

Transition metal-catalyzed cross-coupling reactions have emerged as one of the most powerful tools for the creative construction of both carbon−carbon and carbon−heteroatom bonds, especially in the multistep synthesis of biologically active compounds.[8−10] From the series of typically applied d$^{10}$ metals, Pd-catalyzed transformations have received great interest, due to their excellent chemoselectivity, functional group tolerance, and mild operation conditions, which are of great importance in the synthesis of pharmaceuticals and agrochemicals.[11−14] Among these reactions, the Heck cross-coupling between an aryl halide and an sp$^2$ carbon atom

Received: May 12, 2020
Published: June 9, 2020

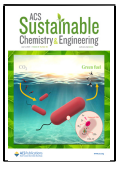

represents a facile protocol to access fine chemicals[15] including complex structures of active pharmaceutical ingredients, for example, montelukast (Merck, antiasthma agent),[16] rilpivirine (Johnson & Johnson, anti-AIDS),[17] eletriptan (Pfizer, antimigraine),[18] and naproxen (Albemarle, anti-inflammatory)[16] (Scheme 1).

**Scheme 1. Pharmaceutical Ingredients Synthesized by the Heck Reaction**[a]

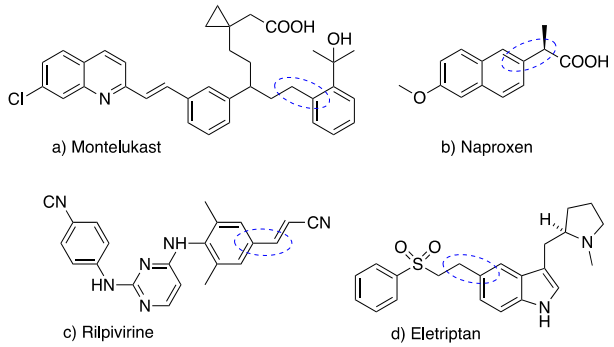


[a]Circled bonds are formed in the Heck reaction.

While the Heck reaction is a commonly utilized transformation and numerous papers focusing on its catalytic aspects have been published, comparatively few studies have appeared on its kinetic investigation. While the elementary steps of the reaction and their sequence in the mechanisms, e.g., (i) oxidative addition,[19] (ii) alkene coordination,[20] (iii) alkene insertion,[21−25] and (iv) reductive elimination,[26] are well-accepted, all of these steps have been proposed to be the rate-determining one. Furthermore, there are limited data regarding the thermodynamic activation parameters. Dupont reported a detailed kinetic study of the reaction of iodobenzene and *n*-butyl-acrylate catalyzed by various palladacycles in DMA. Noteworthy, the postulated mechanism involves the irreversible oxidative addition of iodobenzene to Pd(0) followed by a reversible olefin coordination. An activation enthalpy of $\Delta H^{\ddagger} = 69 \pm 3$ kJ·mol$^{-1}$ and entropy of $\Delta S^{\ddagger} = -43 \pm 8$/J·K$^{-1}$·mol$^{-1}$ were determined for the Pd/$PPh_3$-catalyzed system.[27] Jagtap investigated the $PdCl_2$(bipy)-assisted coupling of styrene and iodobenzene in NMP and determined an activation parameter of $\Delta H^{\ddagger} = 98.7$ kJ·mol$^{-1}$.[28] Amatore determined activation parameters of $\Delta H^{\ddagger} = 75 \pm 5$ kJ·mol$^{-1}$ and an entropy of $\Delta S^{\ddagger} = 7 \pm 8$/J·K$^{-1}$·mol$^{-1}$ for the reaction of iodobenzene and $Pd(PPh_3)_4$ in toluene for the temperature range of 20−50 °C.[29]

Despite numerous advantages, Heck reactions are typically performed in an aprotic, dipolar common organic solvent such as *N*,*N*-dimethylformamide (DMF),[30] *N*-methyl-2-pyrrolidone (NMP),[31] dimethylacetamide (DMA),[32] toluene (Tol),[33] dimethyl sulfoxide (DMSO),[34] 1,4-dioxane (1,4-DO),[35] tetrahydrofuran (THF),[36] or acetonitrile[37] having high toxicity, flammability, vapor pressure, etc. The best solvents for the reaction, i.e., DMF and NMP, are suspected of causing cancer as well. Consequently, the replacement of the reaction medium is crucial to reduce the risk of environmental impact. The application of a nontoxic reaction media is fundamentally important in the pharmaceutical industry, where residual solvent traces can result in serious health issues.

γ-Valerolactone (GVL) was identified as a promising renewable platform molecule by Horváth in 2008,[38] of which several useful applications have been demonstrated.[39−43] It occurs naturally in fruits and fermented products such as wines and beers.[44] GVL can easily be produced from carbohydrate-rich biomass via levulinic acid.[45] Its vapor pressure is much lower than those of conventional organic solvents (Figure 1). It

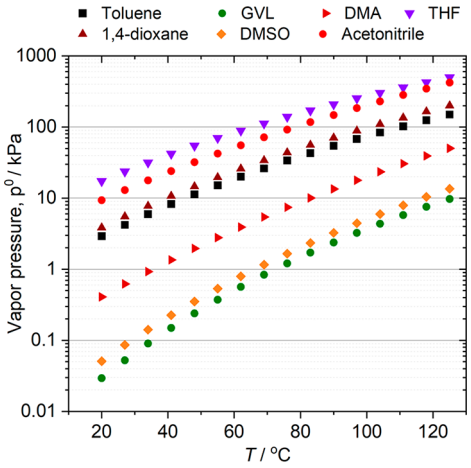


**Figure 1.** Temperature-dependent vapor pressures of selected conventional solvents and GVL. Vapor pressure data were obtained as follows: GVL from ref 50, and THF, 1,4-dioxane, toluene, DMA, acetonitrile, and DMSO from ref 52.

has a good solvating property for many compounds from organic substances to organometallic compounds,[46−49] making it an attractive and a nontoxic ($LD_{50(rat, oral)}$ = 8800 mg/kg)[38] aprotic dipolar reaction medium for the chemical industry. Water, which can seriously affect a catalytic reaction, is completely removed by vacuum distillation.[50,51]

Recently, the successful applications of GVL, as a surrogate of conventional organic solvents, that can contribute to the reduction of VOC emission, which reached 6 million tons in EU28 alone in 2015,[53] were successfully demonstrated. We showed that GVL can be used as a reaction medium for homogeneous hydroformylation[48,54] and aminocarbonylation[55] reactions. Vaccaro pioneered GVL solvent application for several heterogeneous catalytic transformations such as the Heck,[56] Hiyama,[57] and Sonogashira[58] cross-coupling reactions. However, neither the use of GVL in homogeneous cross-coupling reactions nor kinetic study, which is fundamentally important for process modeling, has been reported yet.

Herein we report a catalytic and kinetic study on the homogeneous Pd-catalyzed Heck coupling reaction in γ-valerolactone as an alternative solvent, including investigation of the effect of the catalyst precursor, moisture content of the system, and effect of substituents on the reaction efficiency. A simplified kinetic model was additionally proposed to model the reaction and determine key thermodynamic parameters of the transformation in GVL. The kinetic study was supported by theoretical DFT calculations as well. According to our best knowledge, no comparative kinetically determined thermodynamic parameters were reported on a conventional biomass-based solvent pair.

## EXPERIMENTAL SECTION

Sources of chemicals are listed in Supporting Information. γ-Valerolactone was purified by vacuum distillation[50] and stored under nitrogen before use. Iodobenzene and styrene were purified by vacuum distillation and stored under nitrogen before use. Kinetic


https://dx.doi.org/10.1021/acssuschemeng.0c03523
ACS Sustainable Chem. Eng. 2020, 8, 9926−9936

measurements were performed by the use of iodobenzene and styrene with a purity of >99.95%. Both iodobenzene and styrene derivatives were used as received. The water content of the reaction media was determined by Karl Fischer titration performed with a Hanna Instruments 904.

**General Procedure for the Heck Reaction.** In a 4 mL screw-capped vial, 0.1 mol % (0.224 mg) $Pd(OAc)_2$ was dissolved in 1 mL of water-free GVL followed by the addition of 1 mmol of iodobenzene (**1a**, 204 mg, 113 $\mu$L), 1.2 mmol triethylamine (121 mg, 167 $\mu$L), and 1.2 mmol of styrene (**2a**, 125 mg, 138 $\mu$L). The reaction mixture was heated to the adjusted temperature by a thermostated oil bath and stirred magnetically at 450 rpm. At the given reaction time,10 $\mu$L of reaction mixture sample was taken with a Hamilton syringe and mixed with 1 mL of dichloromethane and 10 $\mu$L of *p*-xylene as an internal standard. The weight of all the components and samples was measured with an analytical balance with readability down to 0.001 g. The qualitative and quantitative analysis were performed by the use of a HP 5890 gas chromatograph equipped with an FID detector and a RESTEK Rtx-5 ms GC column (30 m × 0.25 mm × 0.25 $\mu$m). The FID factors of the corresponding components were calculated to *p*-xylene as follows: iodobenzene (**1a**): 0.771 ± 0.005, styrene (**2a**): 1.000 ± 0.007, *trans*-stilbene (**3a**) and 1,1-diphenylethylene (**4a**): 1.906 ± 0.026.

**Data Treatment.** Evaluation of the concentration−time series measured at different initial iodobenzene (**1a**), styrene (**2a**), and catalyst concentrations was performed with Chemmech program package[59] developed for the comprehensive evaluation of kinetic data to refine the kinetic parameter set of the proposed model by simultaneous data treatment. Regressed parameters of the kinetic model were determined by minimizing the sum of squares of the deviations between the measured and calculated data using a relative fitting procedure option. This means that the deviation between the measured and calculated data was normalized to the largest concentration change in the given experiment and the sum of squares of these was subject to be minimized. The quantitative criterion for an acceptable fit was that the average deviation in the case of all the measured kinetic curves approaches 5%, which was found to be close to the experimentally achievable limit of error. The kinetic curves measured in GVL were obtained by varying $[\text{iodobenzene (1a)}]_0$ = 0.32−0.82 mM, $[\text{styrene (2a)}]_0$ = 0.55−1.3 mM, and $[\text{catalyst}]_0$ = 0.47−1.03 $\mu$M, keeping the rest of the reagent concentrations at constant values. At a fixed initial condition, the kinetic data were measured in the temperature range of 363−393 K. A built-in option of Chemmech program package enables us to determine the activation parameters from the Eyring equation.[60] The temperature dependence of the bimolecular rate-determining step can be given by eq 1, where $T$ is the temperature expressed in Kelvin, and $A = \kappa k_B/\hbar c^{\ominus}$, where $\kappa$ is the transmission factor, $k_B$ and $\hbar$ are the Boltzmann and the Planck constants, respectively, and $c^{\ominus}$ is the standard concentration.[61]

$$k_2 = ATp^{1000/T} \quad (1)$$

The parameter $p$ is defined by eq 2, where $\Delta G^{\ddagger}$ is the activation free energy of the given bimolecular process, and $R$ is the gas constant (8.314472 J·K$^{-1}$·mol$^{-1}$).

$$p = e^{-\Delta G^{\ddagger}/1000R} \quad (2)$$

The fitting process was also executed separately for all the kinetic traces measured in DMF as a solvent simultaneously to compare the parameters obtained with those found in the case of GVL to shed light on the intimate details of the mechanism.

The equations of calculations of conversion, yield, and selectivity are presented in Supporting Information (s1−s5).

**Computational Details.** All the structures were optimized without symmetry constraints with tight convergence criteria using the program ORCA 4.2.1.[62] with the exchange and correlation functionals developed by Grimme[63] containing the D3 empirical dispersion correction with Becke and Johnson damping.[64] For all the atoms, the def2-TZVP basis set[65] was employed with the respective pseudopotentials for palladium and iodine. The stationary points were characterized by frequency calculations to verify that they have zero imaginary frequencies for equilibrium geometries and one imaginary frequency for transition states. Thermochemistry corrections were taken from frequency calculations at 363.15 K and 1 bar. Intrinsic reaction coordinate (IRC) analyses[66] were carried out throughout the reaction pathways to confirm that the stationary points are smoothly connected to each other.

On the optimized geometries, the energies were recomputed with def2-TZVP basis set on all atoms including solvation corrections using the M06 functional[67] and the SMD model, developed by Marenich, Cramer, and Truhlar,[68] with dielectric constants $\varepsilon$ = 30.1 for GVL.[69] This model addresses the problem of solute−solvent interaction: the cavity-dispersion-solvent-structure term was introduced, that arises from short-range interactions between the solute and solvent molecules in the first solvation shell. Additional parameters required for the SMD model were 30.9 for surface tension and 1.443 for the refraction index.[70] For Abraham's hydrogen bond basicity, a value of 0.450 was selected which is used for all types of esters in the SMD library.

## RESULTS AND DISCUSSION

**Catalytic Studies.** We propose that GVL can be an ideal and safe reaction environment for the homogeneous Pd-catalyzed Heck coupling of various iodobenzene and styrene derivatives (Scheme 2). The coupling of 1 mmol of iodobenzene (**1a**) and 1.2 of mmol styrene (**2a**) in the presence of catalysts in situ formed from 0.001 mmol of $Pd(OAc)_2$ and 1.2 mmol of $Et_3N$ in 1 mL of DMF was first performed at 378 K for 30 min,[15,16] as a reference reaction. Moderate conversion (23%) of **1a** with a selectivity of 82% toward *trans*-stilbene (**3a**) was detected. To compare other commonly utilized reaction media to GVL, the coupling of **1a**

**Scheme 2. Heck Coupling Reactions of Substituted Iodobenzene (1a−g) and Styrene (2a−e) Derivatives**

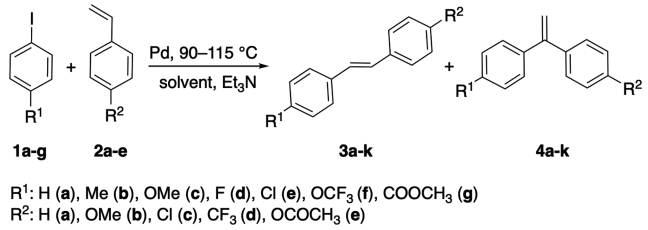


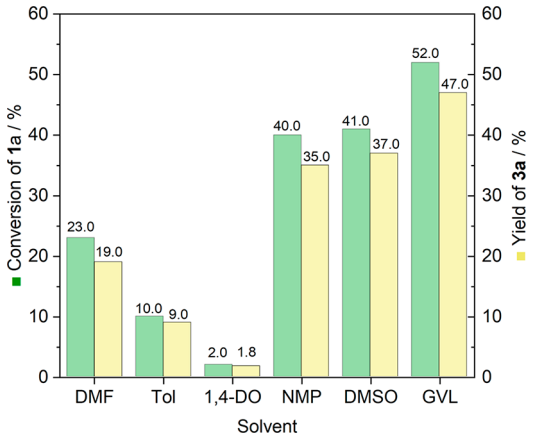


**Figure 2.** Heck coupling of iodobenzene (**1a**) and styrene (**2a**) in different solvents. Reaction conditions: 0.001 mmol of $Pd(OAc)_2$ (0.1 mol %), 1 mmol of **1a**, 1.2 mmol of **2a** of mmol, 1.2 mmol of $Et_3N$, 1 mL of solvent, $t$ = 30 min, $T$ = 378 K.



https://dx.doi.org/10.1021/acssuschemeng.0c03523
ACS Sustainable Chem. Eng. 2020, 8, 9926−9936

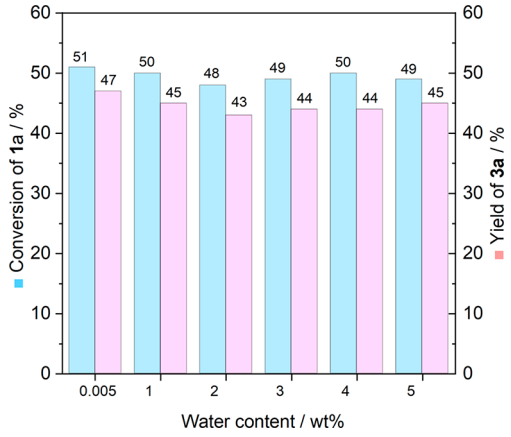


**Figure 3.** Effect of water content on the Heck coupling of iodobenzene (**1a**) and styrene (**2a**). Reaction conditions: 0.001 mmol of $Pd(OAc)_2$ (0.1 mol %), 1 mmol of **1a**, 1.2 mmol of **2a** mmol, 1.2 mmol of $Et_3N$, 1 of mL solvent, $t$ = 30 min, $T$ = 378 K.

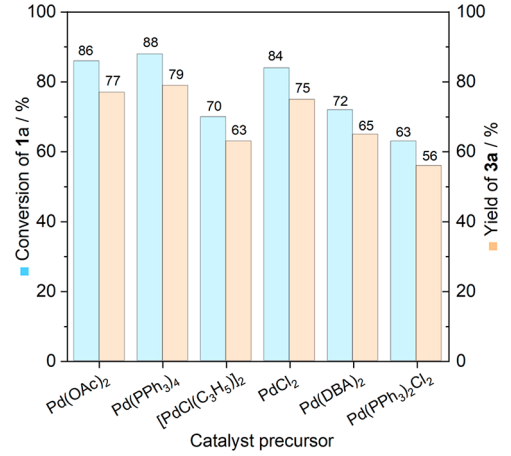


**Figure 4.** Heck coupling of iodobenzene (**1a**) and styrene (**2a**) by the use of different catalyst precursors. Reaction conditions: 0.001 mmol of catalyst precursor, 1 mmol of **1a**, 1.2 mmol of **2a** mmol, 1.2 mmol of $Et_3N$, 1 mL of solvent, $t$ = 30 min, $T$ = 403 K.

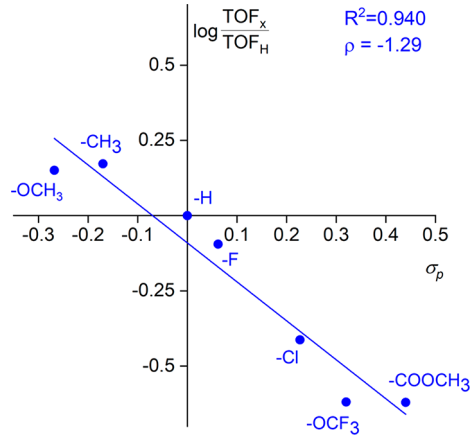


**Figure 5.** $\log(TOF_x/TOF_H)-\sigma_p$ plot for the reaction of iodobenzene (**1a**) and its para-substituted derivatives (**1b–g**) with styrene (**2a**). Reaction conditions: 1.2 mmol of **1a–g**, 1 mmol of **2a**, 1.2 mmol of $Et_3N$, 0.1 mol % of $Pd(OAc)_2$, $T$ = 378 K, $t$ = 30 min. $TOF_x$: turnover frequency of the reaction of **1b–g** at 30 min, $TON_H$: turnover frequency of the reaction of **1a** at 30 min.

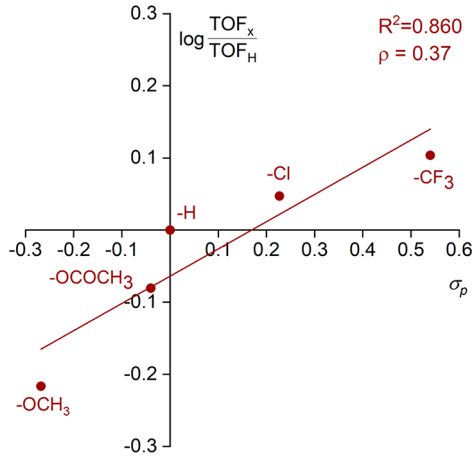


**Figure 6.** $\log(TOF_x/TOF_H)-\sigma_p$ plot for reaction of iodobenzene (**1a**) and styrene (**2a**) and its para-substituted derivatives (**2b–e**). Reaction conditions: 1 mmol of **1a**, 1,2 mmol of **2a–e**, 1.2 mmol of $Et_3N$, 0.1 mol % of $Pd(OAc)_2$, $T$ = 378 K, $t$ = 30 min. $TOF_x$: turnover frequency of the reaction of **2b–e** at 30 min, $TON_H$: turnover frequency of the reaction of **2a** at 30 min.

**Scheme 3. Kinetic Model for Heck Coupling of Iodobenzene (1a) with Styrene (2a) in the Presence of Pd/Triethylamine Catalyst System (C)**

$$\text{IB (1a)} + \text{C} \underset{}{\overset{K_1}{\rightleftharpoons}} \text{IBC} \quad \text{(I)}$$

$$\text{IBC} + \text{S (2a)} \xrightarrow{k_2} \text{IBCS} \quad \text{(II)}$$

$$\text{IBCS} \xrightarrow{k_3\ rapid} \textbf{3a} + \text{C} \quad \text{(III)}$$

$$\text{IBCS} \xrightarrow{k_4\ rapid} \textbf{4a} + \text{C} \quad \text{(IV)}$$

**Table 1. Calculated Parameters for the Proposed Kinetic Model Represented by Eqs I–IV (Scheme 3)**

| solvent | $A$ $(1/(K\cdot s\cdot M^2))$ | $p$ | $k_3/k_4$ |
|---|---|---|---|
| GVL | $(4.11 \pm 0.42) \times 10^{17}$ | $(4.18 \pm 0.39) \times 10^{-6}$ | $9.80 \pm 0.47$ |
| DMF | $(3.42 \pm 0.49) \times 10^{17}$ | $(3.86 \pm 0.41) \times 10^{-6}$ | $8.60 \pm 0.71$ |

and **2a** was repeated in selected fossil-based solvents, i.e., NMP, DMSO, 1,4-DO, and Tol. While marginal conversion rates were detected in Tol and 1,4-DO, significantly higher product formations were observed in NMP and DMSO. By replacing the solvent with GVL, 52% conversion of **1a** with a slightly higher selectivity (90%) of **3a** was observed (Figure 2) under identical conditions. **1a** could be completely converted to **3a** and 1,1-diphenylethylene (**4a**) by applying 2 h reaction time, verifying the successful use of GVL for homogeneous C,C-coupling. Although it was shown that GVL could react with amines, the reactions take place in the presence of mono- and diamines.[43]

The moisture content of a reaction media, which is typically considered as a residual water content after purification of the solvent, could be a critical parameter affecting the formation of catalytically active species, the stability of the catalyst system, formation of byproducts, etc. Because the formation of GVL from 4-hydroxyvaleric acid undergoes an intramolecular esterification reaction, the investigation of the influence of the residual water on the reaction efficiency was essential. The test was performed by the reaction of **1a** and **2a** in the presence of $Pd(OAc)_2/Et_3N$ at 378 K. No decreasing in


https://dx.doi.org/10.1021/acssuschemeng.0c03523
ACS Sustainable Chem. Eng. 2020, 8, 9926–9936

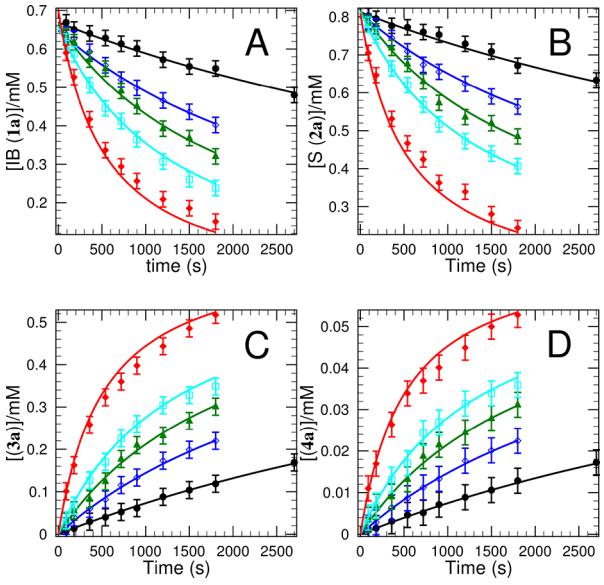


**Figure 7.** Experimental and fitted kinetic curves obtain in the iodobenzene-styrene reaction at different temperature. Initial conditions are as follows: $[\mathbf{1a}]_0$ = 0.67 mM, $[\mathbf{2a}]_0$ = 0.81 mM, $[C]_0$ = 0.7 $\mu$M. $T$ (K) = 363 (black), 373 (blue), 378 (green), 383 (cyan), 393 (red).

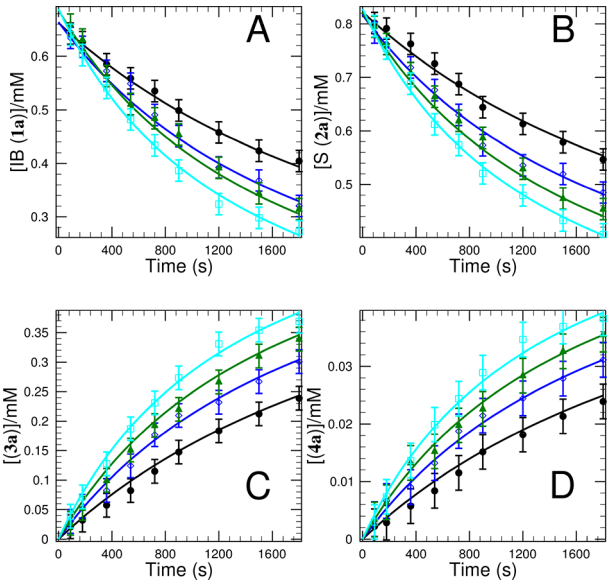


**Figure 8.** Experimental and fitted kinetic curves obtain in the iodobenzene−styrene reaction at different catalyst concentrations. Initial conditions are as follows: $[\mathbf{1a}]_0$ = 0.67 mM, $[\mathbf{2a}]_0$ = 0.81 mM, and $T$ = 378 K. $[C]_0$ ($\mu$M) = 0.47 (black), 0.7 (blue), 0.82 (green), 1.02 (cyan).

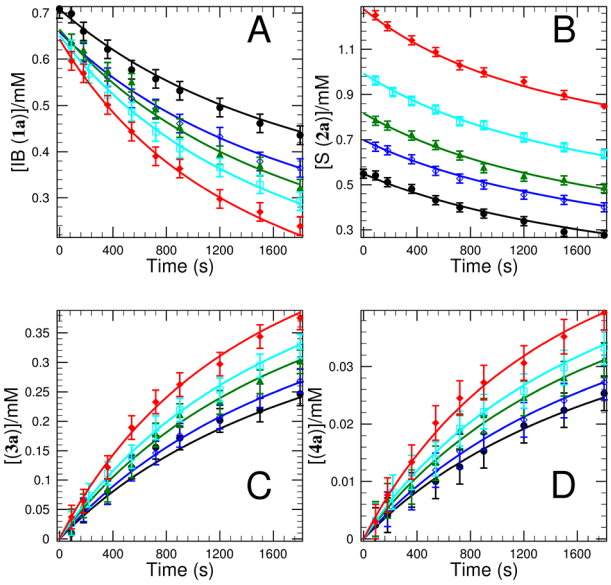


**Figure 9.** Experimental and fitted kinetic curves obtain in the iodobenzene−styrene reaction at different styrene concentrations. Initial conditions are as follows: $[\mathbf{1a}]_0$ = 0.67 mM, $[C]_0$ = 0.68 $\mu$M, and $T$ = 378 K. $[\mathbf{2a}]_0$ (mM) = 0.55 (black), 0.7 (blue), 0.81 (green), 1.0 (cyan), 1.3 (red).

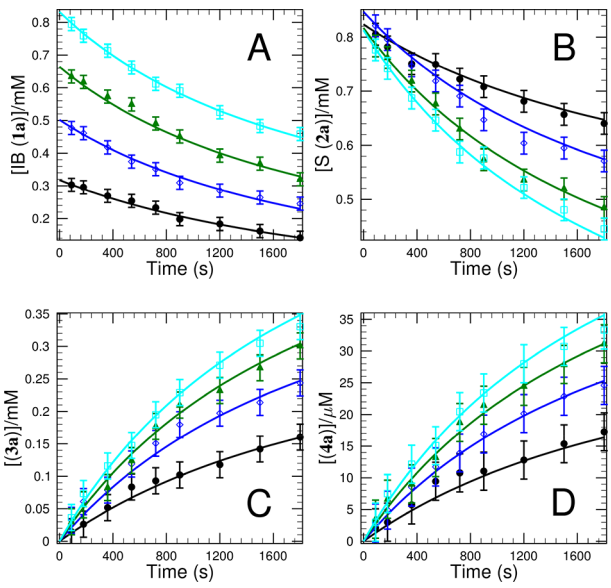


**Figure 10.** Experimental and fitted kinetic curves obtained in the iodobenzene−styrene reaction at different iodobenzene concentrations. Initial conditions are as follows: $[S]_0$ = 0.82 mM, $[C]_0$ = 0.68 $\mu$M, and $T$ = 378 K. $[IB]_0$ (mM) = 0.32 (black), 0.5 (blue), 0.66 (green), 0.83 (cyan).

conversion rates and selectivities were observed when the water content of the reaction mixture was increased up to 5.0 wt %, representing that the method is hardly sensitive for the presence of water (Figure 3). Consequently, no special pretreatment or handling to exclude a small amount of water from the reaction mixture is necessary.

It is well-known that applied catalyst precursors can determine well the formation of catalytically active Pd species.[71] In the absence of tertiary phosphine ligands, which are widely used ligands to stabilize Pd(0) species, the reduction of Pd(II) can be affected by amines, if they are present in the system as a base.[71] In the screening of different Pd salts, i.e., $PdCl_2$, $Pd(OAc)_2$, $Pd(DBA)_2$ (dibenzylideneacetone), $Pd(PPh_3)_2Cl_2$, $[PdCl(C_3H_5)_2]_2$ ($C_3H_5$: allyl), and $Pd(PPh_3)_4$, all were found to be effective precatalysts in the presence of $Et_3N$ (Figure 4), providing excellent rates and selectivities at 403 K (higher temperature compared to solvent screening was selected to obtain higher conversion rates) for 30 min. The use of zerovalent $Pd(DBA)_2$ precursor did not show any increase in the reaction rate, which is in accordance with a previous report.[19]



https://dx.doi.org/10.1021/acssuschemeng.0c03523
ACS Sustainable Chem. Eng. 2020, 8, 9926−9936

Table 2. Calculated $K_1k_2$ Values from the Activation Parameters at Different Temperature for Solvents GVL and DMF

| | $K_1k_2$ ($M^{-2}\cdot s^{-1}$) | | | | |
|---|---|---|---|---|---|
| solvent | 363 K | 373 K | 378 K | 383 K | 393 K |
| GVL | $(2.30 \pm 0.64)\times10^5$ | $(5.90 \pm 1.60)\times10^5$ | $(9.28 \pm 2.48)\times10^5$ | $(1.44 \pm 0.38)\times10^6$ | $(3.37 \pm 0.85)\times10^6$ |
| DMF | $(1.54 \pm 0.50)\times10^5$ | $(3.97 \pm 1.26)\times10^5$ | $(6.25 \pm 1.97)\times10^5$ | $(9.74 \pm 3.05)\times10^5$ | $(2.29 \pm 0.70)\times10^6$ |

Scheme 4. Proposed Formation of the Pd(0) Catalyst from $Pd(OAc)_2$ under Phosphine-Free Conditions

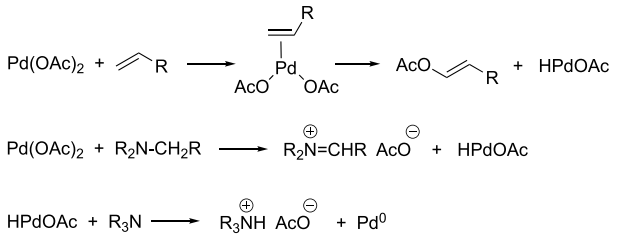


Henceforward, the air-stable and inexpensive $Pd(OAc)_2$ was utilized to facilitate C,C bond coupling involving various iodoaromatic substances (**1b**–**h**) and styrene (**2a**) (Scheme 2) in GVL. Generally, the catalyst system showed excellent functional group tolerance under applied conditions. However, when the electronic property of iodobenzene was varied by changing the para substituent ($\sigma_p$) between $\sigma_{p,OCH3} = -0.268$ and $\sigma_{p,COOCH3} = 0.44$, significant differences in the reaction rates were detected. Figure 5 reveals an acceptable linear correlation ($R^2 = 0.940$) between $\log(TOF_x/TOF_H)$ and $\sigma_p$, where $TOF_x$ is the turnover frequency of the conversion of the corresponding para-substituted iodobenzene, and $TOF_H$ is the turnover frequency of the conversion of iodobenzene (**1a**) at 30 min reaction time. The negative slope value of $\rho = -1.29$ clearly indicates that electron-donating substituents enhance the reactivity of the corresponding aryl halides with catalytically active Pd(0) species via oxidative addition. Similar effects which assume a three-center reaction[72] were reported by Czernecki and co-workers for the Heck reaction.[19] The opposite tendency can be displayed when the para substituent of styrene was replaced. It was shown that the presence of electron-withdrawing substituents enhances the activation of $sp^2$ carbon atoms of olefins (Figure 6) and results in higher TOF values compared to styrene. Although the quality of the correlation is lower ($R^2 = 0.860$) than that of iodobenzene derivatives, a clear rate dependence on $\sigma_p$ can be demonstrated.

**Kinetic Studies.** To clarify the process of the reaction, a detailed kinetic study was performed by the use of the base reaction of iodobenzene (**1a**) and styrene (**2a**) in the temperature range of 363–393 K. It was found that iodobenzene (IB (**1a**)) and styrene (S (**2a**)) in the presence of GVL even at elevated temperature (363–393 K) did not react with each other to a measurable extent. However, in the presence of $Pd(OAc)_2/Et_3N$ catalyst (C) the reaction steadily proceeded, yielding *trans*-stilbene (**3a**) as a major and 1,1-diphenylethylene (**4a**) as a minor product. We propose a simplified model (Scheme 3) to describe the experimentally gathered kinetic data by the variation of concentration of catalyst, **1a**, and **2a** in the range of 0.47–1.02 $\mu$M, 0.32–0.83 $\mu$M, and 0.55–1.03 $\mu$M, respectively, in GVL.

According to the generally accepted mechanism of the Heck reaction,[25,73,82] eq I (Scheme 3) represents a proposed rapid reversible addition of iodobenzene (**1a**) to the catalytically active Pd(0) species, which leads to the formation of complex IBC. It has an auxiliary but small equilibrium constant value ($K_1$), which cannot be determined uniquely under the experimental conditions applied. The subsequent step of the mechanism is the reaction of IBC complex with styrene (**2a**)

Scheme 5. Oxidative Addition Pathways Starting from Styrene and Triethylamine-Ligated Pd(0) Leading to the Key Intermediate Pd(II)(Ph)(I)($NEt_3$) (free energies are given in kJ·mol$^{-1}$ and are relative to complex 7)

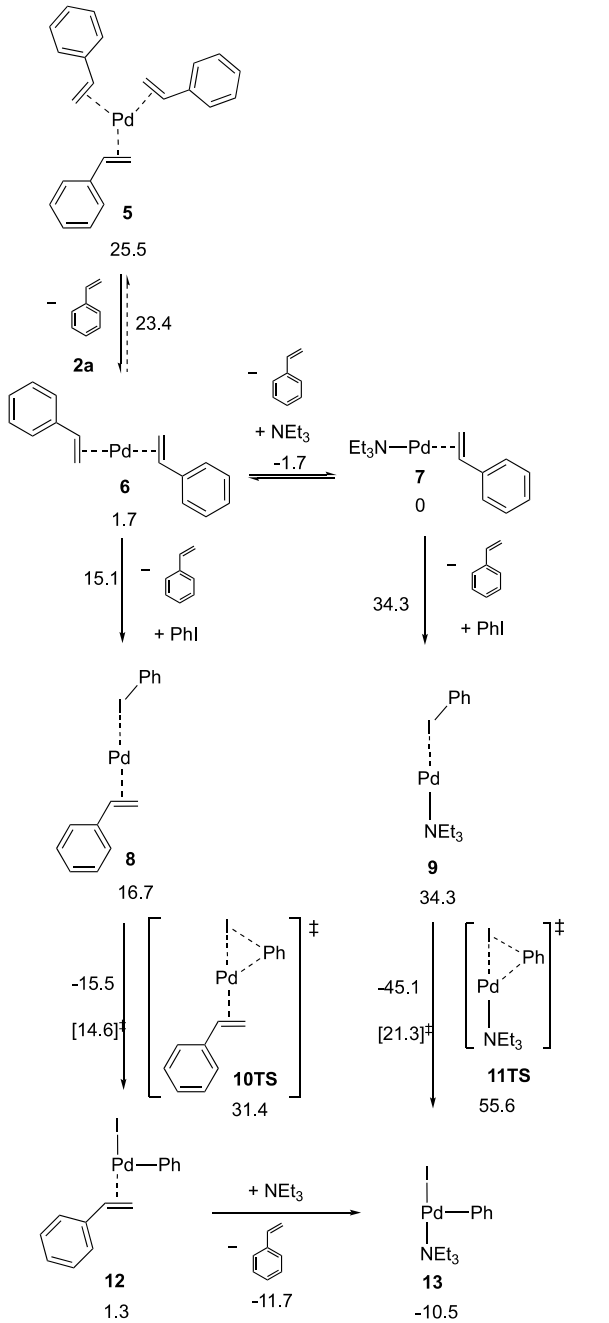




https://dx.doi.org/10.1021/acssuschemeng.0c03523
ACS Sustainable Chem. Eng. 2020, 8, 9926–9936

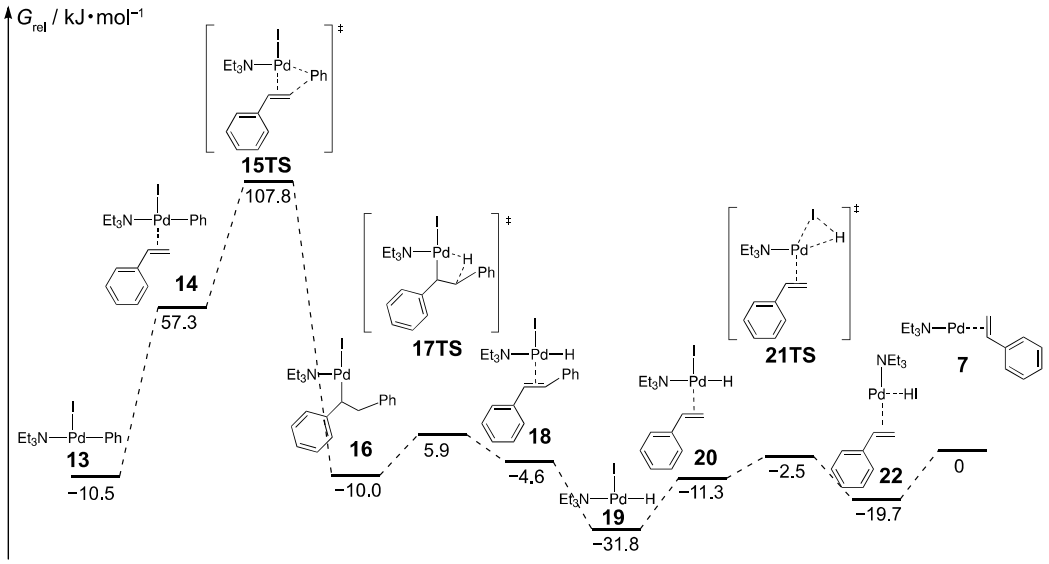


**Figure 11.** Proposed mechanism of the carbon−carbon coupling, $\beta$-elimination, and HI elimination for the linear pathway leading to stilbene. Free energies are given in kJ·mol$^{-1}$ and are relative to complex 7.

(eq II) that can herein be proposed as the rate-determining bimolecular reaction. Therefore, its rate coefficient ($k_2$) can be determined as a primary temperature-dependent kinetic parameter. This suggestion is supported by the experimental fact that the formal kinetic orders of the reactants were determined to be slightly lower than unity (see Supporting Information, Figure S2). This important experimental information, along with the fact that in the absence of catalysts the reactants do not react with each other at a measurable rate even at elevated temperature, means that the reaction has to be initiated by a rapidly established equilibrium between one of the reactants and the catalyst to produce an activated species (IBC) followed by a subsequent process where this intermediate reacts with the substrate molecule (see eq II of Scheme 3). According to these assumptions, the value of $K_1k_2$ can exclusively be determined. Implicitly, any change in the reaction temperature has an effect on both $K_1$ and $k_2$; however, the effect can be interpreted for only $K_1k_2$ from the experimental data set. Thus, the activation parameters determined here can only be treated as overall apparent parameters including not only the activation enthalpy and entropy of the rate-determining step but also an additive term originating from the temperature dependence of the preequilibrium (eq I) as well as the standard enthalpy and entropy changes of the activated complex formation. According to eqs 1 and 2, algebraic manipulation may easily result in eq 3, where $\Delta S^{\ddagger}$/J·K$^{-1}$·mol$^{-1}$ and $\Delta H^{\ddagger}$/J·mol$^{-1}$ are the activation entropy and activation enthalpy of the reaction, and $\Delta S^{\ominus}$/J·K$^{-1}$·mol$^{-1}$ and $\Delta H^{\ominus}$/J·mol$^{-1}$ are the standard entropy and entropy change of the activated complex formation, expressing the $k_2$ second-order rate coefficient. Taking into consideration that $K_1 = \frac{1}{c^{\ominus}} \times e^{-\Delta G_1^{\ominus}/RT}$, where $\Delta G_1^{\ominus}$/J·mol$^{-1}$ is the standard free energy of the IBC complex formation, one may arrive at an expression for $K_1k_2$ by eq 4.

$$k_2 = \left(\frac{\kappa k_B}{\hbar c^{\ominus}} \times e^{(\Delta S^{\ddagger}+\Delta S^{\ominus})/R}\right) T e^{-(\Delta H^{\ddagger}+\Delta H^{\ominus})/RT} \quad (3)$$

$$K_1k_2 = \left(\frac{\kappa k_B}{\hbar (c^{\ominus})^2} \times e^{(\Delta S^{\ddagger}+\Delta S^{\ominus}+\Delta S_1^{\ominus})/R}\right) T e^{-(\Delta H^{\ddagger}+\Delta H^{\ominus}+\Delta H_1^{\ominus})/RT} \quad (4)$$

Comparing eqs 1 and 2 with the one presented above and taking into consideration that Chemmech program package is able to refine parameters $A$ (see eq 1) and $p$ (eq 2), one may easily conclude that the apparent overall activation enthalpy defined as $\Delta H_{app}^{\ddagger} = \Delta H^{\ddagger} + \Delta H^{\ominus} + \Delta H_1^{\ominus}$ may be determined as $\Delta H_{app}^{\ddagger} = R \ln p$, and the result is obtained in kJ·mol$^{-1}$ units. At the same time, the apparent overall activation entropy defined as $\Delta S_{app}^{\ddagger} = \Delta S^{\ddagger} + \Delta S^{\ominus} + \Delta S_1^{\ominus}$ may be calculated from parameter $A$ by eq 5. Furthermore, steps indicated by eqs III and IV are also rapid reactions, and only the ratio of these rate coefficients can be unambiguously calculated from our experimental data. This follows from the fact that we could not find any experimental evidence for intermediate (IBCS) accumulation in a detectable amount. This is the reason why only the $k_3/k_4$ ratio could be calculated from our data and not the individual rate coefficients $k_3$ and $k_4$. Actually, the $k_3/k_4$ ratio refers to the concentration ratio of the products *trans*-stilbene (**3a**) and 1,1-diphenylethylene (**4a**). Parameters calculated from the simultaneous evaluation of the measured data are represented in Table 1.

$$\Delta S_{app}^{\ddagger} = R \ln\left(\frac{A\hbar c^{\ominus 2}}{\kappa k_B}\right) \quad (5)$$

The average deviation for all the kinetic curves measured in GVL solvent was found to be 3.7%, while in the case of DMF it was 5.3%, indicating a sound agreement between the measured and calculated data. Representative measured and calculated data are shown in Figures 7−10. It was clearly demonstrated that the kinetic model with calculated parameters can describe the experimental data points. For the sake of clarity, $K_1k_2$ values are also shown in Table 2 at different temperatures for solvents GVL and DMF.

The data presented in Table 1 lead to the $\Delta H_{app}^{\ddagger}$ = +103.0 kJ·mol$^{-1}$ for the apparent overall activation enthalpy of the reaction when GVL is used as a solvent and $\Delta H_{app}^{\ddagger}$ = +103.7 kJ·


https://dx.doi.org/10.1021/acssuschemeng.0c03523
ACS Sustainable Chem. Eng. 2020, 8, 9926−9936

$mol^{-1}$ in case of DMF. These values show excellent agreement with those determined by Jagtap and co-workers (+98.7 kJ·$mol^{-1}$) using NMP as a solvent.[28] At the same time $\Delta S^{\ddagger}_{app}$ = +139.7 J·$mol^{-1}$·$K^{-1}$ can be calculated for the apparent overall activation entropy of the reaction in the presence of GVL, and $\Delta S^{\ddagger}_{app}$ = +138.1 J·$mol^{-1}$·$K^{-1}$ in the presence of DMF. According to our best knowledge, no comparative kinetically determined thermodynamic parameters were reported on a conventional and a biomass-based solvent pair. These apparent activation parameters and the reasonably close-fitted value for $k_3/k_4$ ratio support that the medium does not play any crucial role in the reaction mechanism. The positive value obtained for the apparent overall activation entropy may seem to be unforeseen if one considers that the rate-determining step of the reaction is association. As, however, eq 4 clearly shows, this apparent contradiction may easily be reconciled by the fact that the apparent activation parameter also includes the standard enthalpy and entropy changes of the adduct IBC and those of the activated complex as well-meaning that the actual activation entropy may readily be a negative value over-compensated by positive values of $\Delta S^{\ominus}_{1}$ and $\Delta S^{\ominus}$.

**Computational Studies.** The mechanism of the Heck reaction has been the subject of numerous theoretical studies. Most of them examined the catalytic pathways with phosphine ligands,[74−76] with phosphine-free systems,[77−80] or both possibilities.[81] Depending on the reaction conditions, the reaction can follow either a neutral or a cationic pathway. Even under phosphine-free conditions and when only the neutral pathway is considered, there are a few possible candidates for catalytically active Pd(0) species. For coordinating ligands, styrene and trimethylamine are both available under proper reaction conditions. In the presence of phosphines, the reduction of Pd(II) to Pd(0) takes place via the oxidation of 1 equiv of phosphine. As reducing agents, however, olefins and amines are appropriate as well. In these cases, the intermediate species is HPdOAc, which acts as a Brønsted acid protonating the triethylamine (Scheme 4) followed by the release of a quaternary ammonium salt with $[OAc]^-$ anion and a Pd(0) species which can accommodate amines or olefins.[82]

To check the applicability of $NEt_3$ as ligand, some reactions were repeated replacing triethylamine with inorganic bases, such as potassium carbonate or cesium carbonate. The substantial drop in the conversion seems to confirm that $NEt_3$ plays an important role in the catalytic activity.

In contrast to the vast number of Pd(0)−monophosphine complexes, zerovalent palladium species containing monodentate nitrogen ligands had not been described until 2003 when novel $Pd(0)(NR_3)_2(ma)$ types of complexes (ma = maleic anhydride) were reported.[83]

Scheme 5 displays the ligand interchange reactions between two- and three-coordinate Pd(0)−styrene complexes and the replacement of one styrene by triethylamine. A recent computational report suggests that 2 or even 3 equiv of styrene is feasible as coordinating ligands;[84] thus, the initial point of our ligand exchange pathways is the ligand dissociation from $Pd(styrene)_3$ (**5**) resulting in the 14-electron $Pd(styrene)_2$ complex (**6**) that is exergonic by 23.4 kJ·$mol^{-1}$. The exchange of one styrene ligand for $NEt_3$, resulting in **7**, is slightly preferred, as the Gibbs free energy change is −1.7 kJ·$mol^{-1}$.

For the reaction of iodobenzene with **6** or **7**, one styrene ligand is replaced by PhI which coordinates in a $\eta^1$ manner affording complex **8** or **9** with a free energy change of 16.7 or 34.3 kJ· $mol^{-1}$, respectively. The oxidative addition is notably faster in the case of styrene as ligand. The combined process leading to the Pd(II) complexes Pd(styrene)(I)(Ph) or $Pd(NEt_3)(I)(Ph)$ takes place with a free energy barrier of 31.4 kJ·$mol^{-1}$ for the former and 55.6 kJ·$mol^{-1}$ for the latter case with respect to **7**. Among the Pd(II)complexes, the ligand exchange from styrene to triethylamine is preferred thermodynamically by −11.7 kJ·$mol^{-1}$.

Figure 11 depicts the remainder of the reaction mechanism starting from the relatively stable complex. Here only the major reaction channel that is the one which leads to stilbene was taken into consideration. The coupling step occurs first with the recoordination of styrene followed by the formation of a new carbon−carbon bond leading to the alkyl complex **16** from **14** via the transition state **15TS**. This combined step is an equilibrium process with a barrier of 118.4 kJ·$mol^{-1}$. Significantly faster is the subsequent $\beta$-elimination affording the coordinated stilbene via **17TS** (15.9 kJ·$mol^{-1}$). Complex **18** rapidly loses stilbene, resulting in the coordinatively unsaturated iodo-hydride species **19**. The overall elimination step is exergonic by −21.8 kJ·$mol^{-1}$. Endergonic coordination of styrene leads to complex **20**, and the rapid and slightly endergonic (by 12.1 kJ·$mol^{-1}$) coupling of the hydrido and iodo ligands results in adduct **22** via transition state **21TS** which affords the catalytically active complex **7**. For the computational modeling, the role of the base in the HI elimination was omitted, but it is reasonable to assume that the assistance of the base opens a pathway with an even lower barrier.

The pathway outlined above is one possible pathway describing the Heck reaction under the reaction condition applied. The agreement with the kinetic measurements, however, suggests the involvement of triethylamine as spectator and styrene as both spectator and coordinating ligand in the catalytic cycle. Moreover, it can be safely concluded that the rate-determining step is the coupling of the coordinated phenyl group to the terminal carbon of styrene.

To check whether the computationally obtained substituent effects agree with the experimental observations, transition state **15TS** was recomputed with one electron-donating ($OCH_3$) and one electron-withdrawing ($OCF_3$) substituent. The free energy barrier is 116.3 and 122.2 kJ·$mol^{-1}$, respectively, when the substituents are placed on the phenyl ring at the 4-position. Thus, in accordance with the trends established by the experimental TOFs, the calculations show that 4-substituents with negative Hammett constants on iodobenzene increase whereas positive constants decrease the reaction rate for the catalytic system containing styrenes and triethylamine.

## CONCLUSIONS

It was demonstrated that $\gamma$-valerolactone can be utilized as a biomass-originated, renewable aprotic dipolar reaction medium for the homogeneous Pd-catalyzed Heck coupling reaction. The reaction shows remarkable tolerance for the moisture content of the reaction mixture and gives good efficiency for Pd(II) catalyst precursors such as $PdCl_2$, $Pd(OAc)_2$, and $Pd(PPh_3)_4$. In addition, the catalyst system shows excellent functional group tolerance. It was revealed that the electron-withdrawing para substituents of iodoaromatic substances accelerate the activity of corresponding species. An opposite tendency was shown for styrene derivatives. A simplified kinetic model was found to model the transformation, which


https://dx.doi.org/10.1021/acssuschemeng.0c03523
ACS Sustainable Chem. Eng. 2020, 8, 9926−9936

can be represented by excellent fitting of the calculated concentration of corresponding species on the experimentally determined points. $\Delta H^{\ddagger}_{app}$ = 103.0 kJ·mol$^{-1}$ for the apparent overall activation enthalpy of the reaction in GVL and $\Delta H^{\ddagger}_{app}$ = 103.7 kJ·mol$^{-1}$ in the case of DMF were determined. Similarly, $\Delta S^{\ddagger}_{app}$ = +139.7 J·mol$^{-1}$·K$^{-1}$ was calculated for the apparent overall activation entropy of the reaction in the presence of GVL, and $\Delta S^{\ddagger}_{app}$ = +138.1 J·mol$^{-1}$·K$^{-1}$ in the presence of DMF. According to our best knowledge, no comparative kinetically determined thermodynamic parameters have been reported on a conventional biomass-based solvent pair. Our computational study confirmed the experimentally observed trends regarding the effect of electron-donating and -withdrawing substituents of iodobenzene and styrene as follows: the electron-donating substituents accelerate the reaction rate for iodobenzene and but decrease the reactivity for styrene derivatives.

## ■ ASSOCIATED CONTENT

### Supporting Information

The Supporting Information is available free of charge at https://pubs.acs.org/doi/10.1021/acssuschemeng.0c03523.

Source of chemicals, experimental and fitted kinetic curves for Heck reaction in DMF (Figure S1), results of the initial rate studies (Figure S2), calculations of conversion, yields, and selectivities (s1−s4), structures of transition states (Figure S3), and Cartesian coordinates, absolute Gibbs free energies, and number of imaginary frequencies ($N_{imag}$) of optimized structures occurring in this study (Table S1) (PDF)

## ■ AUTHOR INFORMATION


### Corresponding Authors

**László T. Mika** − *Department of Chemical and Environmental Process Engineering, Budapest University of Technology and Economics, Budapest H-1111, Hungary;* orcid.org/0000-0002-8520-0065; Email: laszlo.t.mika@mail.bme.hu

**Attila K. Horváth** − *Department of Inorganic Chemistry, Institute of Chemistry, Faculty of Sciences, University of Pécs, Pécs H-7624, Hungary;* orcid.org/0000-0002-1916-2451; Email: horvatha@gamma.ttk.pte.hu

### Authors

**Dániel Fodor** − *Department of Chemical and Environmental Process Engineering, Budapest University of Technology and Economics, Budapest H-1111, Hungary*

**Tamás Kégl** − *Department of Inorganic Chemistry and MTA-PTE Research Group for Selective Chemical Syntheses, University of Pécs, Pécs H-7624, Hungary;* orcid.org/0000-0002-4642-1703

**József M. Tukacs** − *Department of Chemical and Environmental Process Engineering, Budapest University of Technology and Economics, Budapest H-1111, Hungary*

Complete contact information is available at: https://pubs.acs.org/10.1021/acssuschemeng.0c03523


### Notes

The authors declare no competing financial interest.

## ■ ACKNOWLEDGMENTS

This work was funded by National Research, Development and Innovation Office − NKFIH (KH 129508) and Higher Education Excellence Program of the Ministry of Human Capacities in the frame of biotechnology research area of Budapest University of Technology and Economics (BME FIKP-BIO) and in the framework of the innovation for sustainable and healthy living and environment thematic program of the University of Pécs. A. K. Horváth is thankful for support of a GINOP-2.3.2-15-2016-00049 grant. L. T. Mika is grateful for the support of Scholarship of József Varga Foundation, Budapest University of Technology and Economics, Budapest, Hungary.

## ■ ABBREVIATIONS

DBA, dibenzylideneacetone; DFT, density functional theory; DMF, *N*,*N*-dimethylformamide; 1,4-DO, 1,4-dioxane; GVL, γ-valerolactone; DMSO, dimethyl sulfoxide; NMP, *N*-methyl-2-pyrrolidone; THF, tetrahydrofuran; Tol, toluene; DMA, dimethylacetamide; TOF, turnover frequency; TS, transition state

## ■ REFERENCES


(1) Náray-Szabó, G.; Mika, L. T. Conservative Evolution and Industrial Metabolism in Green Chemistry. *Green Chem.* **2018**, *20*, 2171−2191.

(2) Horváth, I. T.; Anastas, P. T. Innovations and Green Chemistry. *Chem. Rev.* **2007**, *107*, 2169−2173.

(3) Erythropel, H. C.; Zimmerman, J. B.; de Winter, T. M.; Petitjean, L.; Melnikov, F.; Lam, C. H.; Lounsbury, A. W.; Mellor, K. E.; Janković, N. Z.; Tu, Q.; et al. The Green ChemisTREE: 20 Years After Taking Root with the 12 Principles. *Green Chem.* **2018**, *20*, 1929−1961.

(4) Horváth, I. T. Introduction: Sustainable Chemistry. *Chem. Rev.* **2018**, *118*, 369−371.

(5) Sheldon, R. A. Green and Sustainable Manufacture of Chemicals From Biomass: State of the Art. *Green Chem.* **2014**, *16*, 950−963.

(6) *BP Statistical Review of World Energy June 2019*, 68th ed.; https://www.bp.com/en/global/corporate/energy-economics/statistical-review-of-world-energy.html (accessed November 20, 2019).

(7) Shi, W.; Liu, C.; Lei, A. Transition-Metal Catalyzed Oxidative Cross-Coupling Reactions to Form C-C Bonds Involving Organometallic Reagents as Nucleophiles. *Chem. Soc. Rev.* **2011**, *40*, 2761−2776.

(8) Clark, J.; Farmer, T.; Hunt, A.; Sherwood, J. Opportunities for Bio-Based Solvents Created as Petrochemical and Fuel Products Transition Towards Renewable Resources. *Int. J. Mol. Sci.* **2015**, *16*, 17101−17159.

(9) Yang, Y.; Lan, J.; You, J. Oxidative C-H/C-H Coupling Reactions Between Two (Hetero)Arenes. *Chem. Rev.* **2017**, *117*, 8787−8863.

(10) Jana, R.; Pathak, T. P.; Sigman, M. S. Advances in Transition Metal (Pd, Ni, Fe)-Catalyzed Cross-Coupling Reactions Using Alkyl-Organometallics as Reaction Partners. *Chem. Rev.* **2011**, *111*, 1417−1492.

(11) Devendar, P.; Qu, R.-Y.; Kang, W.-M.; He, B.; Yang, G.-F. Palladium-Catalyzed Cross-Coupling Reactions: a Powerful Tool for the Synthesis of Agrochemicals. *J. Agric. Food Chem.* **2018**, *66*, 8914−8934.

(12) Tarnowicz-Ligus, S.; Trzeciak, A. Heck Transformations of Biological Compounds Catalyzed by Phosphine-Free Palladium. *Molecules* **2018**, *23*, 2227−2237.

(13) Le Bras, J.; Muzart, J. Intermolecular Dehydrogenative Heck Reactions. *Chem. Rev.* **2011**, *111*, 1170−1214.

(14) Torborg, C.; Beller, M. Recent Applications of Palladium-Catalyzed Coupling Reactions in the Pharmaceutical, Agrochemical, and Fine Chemical Industries. *Adv. Synth. Catal.* **2009**, *351*, 3027−3043.

(15) Jagtap, S. Heck Reaction—State of the Art. *Catalysts* **2017**, *7*, 267−53.

(16) De Vries, J. G. The Heck Reaction in the Production of Fine Chemicals. *Can. J. Chem.* **2001**, *79*, 1086−1092.
(17) Biffis, A.; Centomo, P.; Del Zotto, A.; Zecca, M. Pd Metal Catalysts for Cross-Couplings and Related Reactions in the 21st Century: a Critical Review. *Chem. Rev.* **2018**, *118*, 2249−2295.
(18) Madasu, S. B.; Vekariya, N. A.; Kiran, M. N. V. D. H.; Gupta, B.; Islam, A.; Douglas, P. S.; Babu, K. R. Synthesis of Compounds Related to the Anti-Migraine Drug Eletriptan Hydrobromide. *Beilstein J. Org. Chem.* **2012**, *8*, 1400−1405.
(19) Benhaddou, R.; Czernecki, S.; Ville, G.; Zegar, A. A Kinetic Investigation of Some Electronic Factors and Ligand Effects in the Heck Reaction with Allylic Alcohols. *Organometallics* **1988**, *7*, 2435−2439.
(20) Rosner, T.; Le Bars, J.; Pfaltz, A.; Blackmond, D. G. Kinetic Studies of Heck Coupling Reactions Using Palladacycle Catalysts: Experimental and Kinetic Modeling of the Role of Dimer Species. *J. Am. Chem. Soc.* **2001**, *123*, 1848−1855.
(21) Ohff, M.; Ohff, A.; Van der Boom, M. E.; Milstein, D. Highly Active Pd(II) PCP-Type Catalysts for the Heck Reaction. *J. Am. Chem. Soc.* **1997**, *119*, 11687−11688.
(22) Jutand, A. The Use of Conductivity Measurements for the Characterization of Cationic Palladium(II) Complexes and for the Determination of Kinetic and Thermodynamic Data in Palladium-Catalyzed Reactions. *Eur. J. Inorg. Chem.* **2003**, *2003*, 2017−2040.
(23) Van Strijdonck, G. P. F.; Boele, M. D. K.; Kamer, P. C. J.; de Vries, J. G.; van Leeuwen, P. W. N. M. Fast Palladium Catalyzed Arylation of Alkenes Using Bulky Monodentate Phosphorus Ligands. *Eur. J. Inorg. Chem.* **1999**, *7*, 1073−1076.
(24) Albéniz, A. C.; Espinet, P.; Martín-Ruiz, B.; Milstein, D. Catalytic System for Heck Reactions Involving Insertion Into Pd-(Perfluoro-Organyl) Bonds. *J. Am. Chem. Soc.* **2001**, *123*, 11504−11505.
(25) Schmidt, A. F.; Al-Halaiqa, A.; Smirnov, V. V. Heck Reactions of Alkenes with Aryl Iodides and Aryl Bromides: Rate-Determining Steps Deduced From a Comparative Kinetic Study of Competing and Noncompeting Reactions. *Kinet. Catal.* **2007**, *48*, 716−727.
(26) Shmidt, A. F.; Smirnov, V. V. Oxidative Addition Step in Reactions Involving Palladium Activation of Carbon-Halogen and Carbon-Oxygen Bonds. *Kinet. Catal.* **2005**, *46*, 495−501.
(27) Consorti, C. S.; Flores, F. R.; Dupont, J. Kinetics and Mechanistic Aspects of the Heck Reaction Promoted by a CN-Palladacycle. *J. Am. Chem. Soc.* **2005**, *127*, 12054−12065.
(28) Jagtap, S. V.; Deshpande, R. M. Insight Into $PdCl_2$(Bipy) Complex as an Efficient Catalyst for Heck Reaction and Kinetic Investigations in Homogeneous Medium. *Kinet. Catal.* **2013**, *54*, 314−321.
(29) Amatore, C.; Pflüger, F. Mechanism of Oxidative Addition of Palladium(0) with Aromatic Iodides in Toluene, Monitored at Ultramicroelectrodes. *Organometallics* **1990**, *9*, 2276−2282.
(30) Kantam, M. L.; Srinivas, P.; Yadav, J.; Likhar, P. R.; Bhargava, S. Trifunctional N, N, O-Terdentate Amido/Pyridyl Carboxylate Ligated Pd(II) Complexes for Heck and Suzuki Reactions. *J. Org. Chem.* **2009**, *74*, 4882−4885.
(31) Kantchev, E. A. B.; Peh, G.-R.; Zhang, C.; Ying, J. Y. Practical Heck-Mizoroki Coupling Protocol for Challenging Substrates Mediated by an N-Heterocyclic Carbene-Ligated Palladacycle. *Org. Lett.* **2008**, *10*, 3949−3952.
(32) Wang, G.-Z.; Shang, R.; Fu, Y. Irradiation-Induced Palladium-Catalyzed Decarboxylative Heck Reaction of Aliphatic N-(Acyloxy)-Phthalimides at Room Temperature. *Org. Lett.* **2018**, *20*, 888−891.
(33) Dong, X.; Han, Y.; Yan, F.; Liu, Q.; Wang, P.; Chen, K.; Li, Y.; Zhao, Z.; Dong, Y.; Liu, H. Palladium-Catalyzed 6-Endo Selective Alkyl-Heck Reactions: Access to 5-Phenyl-1,2,3,6-Tetrahydropyridine Derivatives. *Org. Lett.* **2016**, *18*, 3774−3777.
(34) Hartung, C. G.; Köhler, K.; Beller, M. Highly Selective Palladium-Catalyzed Heck Reactions of Aryl Bromides with Cycloalkenes. *Org. Lett.* **1999**, *1*, 709−711.
(35) Littke, A. F.; Fu, G. C. Heck Reactions in the Presence of P(T-Bu) 3: Expanded Scope and Milder Reaction Conditions for the Coupling of Aryl Chlorides. *J. Org. Chem.* **1999**, *64*, 10−11.
(36) Shaikh, T. M.; Hong, F.-E. Palladium(II)-Catalyzed Heck Reaction of Aryl Halides and Arylboronic Acids with Olefins Under Mild Conditions. *Beilstein J. Org. Chem.* **2013**, *9*, 1578−1588.
(37) Ziegler, F. E.; Chakraborty, U. R.; Weisenfeld, R. B. A Palladium-Catalyzed Carbon-Carbon Bond Formation of Conjugated Dienones: a Macrocyclic Dienone Lactone Model for the Carbomycins. *Tetrahedron* **1981**, *37*, 4035−4040.
(38) Horváth, I. T.; Mehdi, H.; Fábos, V.; Boda, L.; Mika, L. T. Γ-Valerolactone—a Sustainable Liquid for Energy and Carbon-Based Chemicals. *Green Chem.* **2008**, *10*, 238−242.
(39) Mehdi, H.; Fábos, V.; Tuba, R.; Bodor, A.; Mika, L. T.; Horváth, I. T. Integration of Homogeneous and Heterogeneous Catalytic Processes for a Multi-Step Conversion of Biomass: From Sucrose to Levulinic Acid, Γ-Valerolactone, 1,4-Pentanediol, 2-Methyl-Tetrahydrofuran, and Alkanes. *Top. Catal.* **2008**, *48*, 49−54.
(40) Bond, J. Q.; Alonso, D. M.; Wang, D.; West, R. M.; Dumesic, J. A. Integrated Catalytic Conversion of Γ-Valerolactone to Liquid Alkenes for Transportation Fuels. *Science* **2010**, *327*, 1110−1114.
(41) Cséfalvay, E. Evaluation of Biobased Lighter Fluids. *ACS Sustainable Chem. Eng.* **2018**, *6*, 8417−8426.
(42) Yang, Y.; Wei, X.; Zeng, F.; Deng, L. Efficient and Sustainable Transformation of Gamma-Valerolactone Into Nylon Monomers. *Green Chem.* **2016**, *18*, 691−694.
(43) Chalid, M.; Heeres, H. J.; Broekhuis, A. A. Ring-Opening of Γ-Valerolactone with Amino Compounds. *J. Appl. Polym. Sci.* **2012**, *123*, 3556−3564.
(44) Izquierdo-Cañas, P. M.; Mena-Morales, A.; García-Romero, E. Malolactic Fermentation Before or During Wine Aging in Barrels. *LWT - Food Science and Technology* **2016**, *66*, 468−474.
(45) Mika, L. T.; Cséfalvay, E.; Németh, Á. Catalytic Conversion of Carbohydrates to Initial Platform Chemicals: Chemistry and Sustainability. *Chem. Rev.* **2018**, *118*, 505−613.
(46) Fábos, V.; Mika, L. T.; Horváth, I. T. Selective Conversion of Levulinic and Formic Acids to Γ-Valerolactone with the Shvo Catalyst. *Organometallics* **2014**, *33*, 181−187.
(47) Tukacs, J. M.; Novák, M.; Dibó, G.; Mika, L. T. An Improved Catalytic System for the Reduction of Levulinic Acid to Γ-Valerolactone. *Catal. Sci. Technol.* **2014**, *4*, 2908−2912.
(48) Pongrácz, P.; Kollár, L.; Mika, L. T. A Step Towards Hydroformylation Under Sustainable Conditions: Platinum-Catalysed Enantioselective Hydroformylation of Styrene in Gamma-Valerolactone. *Green Chem.* **2016**, *18*, 842−847.
(49) Tian, X.; Yang, F.; Rasina, D.; Bauer, M.; Warratz, S.; Ferlin, F.; Vaccaro, L.; Ackermann, L. C-H Arylations of 1,2,3-Triazoles by Reusable Heterogeneous Palladium Catalysts in Biomass-Derived γ-Valerolactone. *Chem. Commun.* **2016**, *52*, 9777−9780.
(50) Havasi, D.; Mizsey, P.; Mika, L. T. Vapor-Liquid Equilibrium Study of the Gamma-Valerolactone-Water Binary System. *J. Chem. Eng. Data* **2016**, *61*, 1502−1508.
(51) Havasi, D.; Farkas, D.; Mika, L. T. Isobaric Vapor-Liquid Equilibria of Binary Mixtures of γ-Valerolactone + Acetone and Ethyl Acetate. *J. Chem. Eng. Data* **2020**, *65*, 419−425.
(52) Vapor pressure data were obtained from *Database of ChemCAD - Chemical Process Simulaton Software ver. 7.1.5.11490*; Chemstations, Inc., 2018.
(53) http://ec.europa.eu/eurostat/statistics-explained/index.php/Air_pollution_statistics (accessed on July 10, 2019).
(54) Pongrácz, P.; Bartal, B.; Kollár, L.; Mika, L. T. Rhodium-Catalyzed Hydroformylation in Gamma-Valerolactone as a Biomass-Derived Solvent. *J. Organomet. Chem.* **2017**, *847*, 140−145.
(55) Marosvölgyi-Haskó, D.; Lengyel, B.; Tukacs, J. M.; Kollár, L.; Mika, L. T. Application of γ-valerolactone as an alternative biomass-based medium for aminocarbonylation reactions. *ChemPlusChem* **2016**, *81*, 1224−1229.
(56) Strappaveccia, G.; Ismalaj, E.; Petrucci, C.; Lanari, D.; Marrocchi, A.; Drees, M.; Facchetti, A.; Vaccaro, L. A Biomass-


https://dx.doi.org/10.1021/acssuschemeng.0c03523
*ACS Sustainable Chem. Eng.* 2020, 8, 9926−9936

Derived Safe Medium to Replace Toxic Dipolar Solvents and Access Cleaner Heck Coupling Reactions. *Green Chem.* **2015**, *17*, 365−372.
(57) Ismalaj, E.; Strappaveccia, G.; Ballerini, E.; Elisei, F.; Piermatti, O.; Gelman, D.; Vaccaro, L. Valerolactone as a Renewable Dipolar Aprotic Solvent Deriving From Biomass Degradation for the Hiyama Reaction. *ACS Sustainable Chem. Eng.* **2014**, *2*, 2461−2464.
(58) Strappaveccia, G.; Luciani, L.; Bartollini, E.; Marrocchi, A.; Pizzo, F.; Vaccaro, L. Valerolactone as an Alternative Biomass-Derived Medium for the Sonogashira Reaction. *Green Chem.* **2015**, *17*, 1071−1076.
(59) Peintler, G. *Chemmech, A Comprehensive Program Package for Fitting Parameters of Chemical Reaction Mechanisms*; University of Szeged, Szeged, Hungary, 1989−2017.
(60) Eyring, H. The Activated Complex in Chemical Reactions. *J. Chem. Phys.* **1935**, *3*, 107−115.
(61) Lente, G. *Deterministic Kinetics in Chemistry and Systems Biology, The Dynamics of Complex Reaction Networks*; Springer, 2015.
(62) Neese, F. The ORCA program system. *Wiley Interdiscip. Rev.: Comput. Mol. Sci.* **2012**, *2*, 73−78.
(63) Grimme, S. Accurate description of van der Waals complexes by density functional theory including empirical corrections. *J. Comput. Chem.* **2004**, *25*, 1463−1473.
(64) Grimme, S.; Ehrlich, S.; Goerigk, L. Effect of the Damping Function in Dispersion Corrected Density Functional Theory. *J. Comput. Chem.* **2011**, *32*, 1456−1465.
(65) Weigend, F.; Ahlrichs, R. Balanced basis sets of split valence, triple zeta valence and quadruple zeta valence quality for H to Rn: Design and assessment of accuracy. *Phys. Chem. Chem. Phys.* **2005**, *7*, 3297−3305.
(66) Gonzalez, C.; Schlegel, H. B. An improved algorithm for reaction path following. *J. Chem. Phys.* **1989**, *90*, 2154−2161.
(67) Zhao, Y.; Truhlar, D. A new local density functional for main-group thermochemistry, transition metal bonding, thermochemical kinetics, and noncovalent interactions. *J. Chem. Phys.* **2006**, *125*, 194101−194118.
(68) Marenich, A. V.; Cramer, C. J.; Truhlar, D. G. Universal Solvation Model Based on Solute Electron Density and on a Continuum Model of the Solvent Defined by the Bulk Dielectric Constant and Atomic Surface Tensions. *J. Phys. Chem. B* **2009**, *113*, 6378−6396.
(69) Aparicio, S.; Alcalde, R. Characterization of Two Lactones in Liquid Phase: an Experimental and Computational Approach. *Phys. Chem. Chem. Phys.* **2009**, *11*, 6455−6467.
(70) Fornefeld-Schwarz, U. M.; Svejda, P. Refractive Indices and Relative Permittivities of Liquid Mixtures of Γ-Butyrolactone, Γ-Valerolactone, Δ-Valerolactone, or E-Caprolactone + Benzene, + Toluene, or + Ethylbenzene at 293.15 and 313.15 K and Atmospheric Pressure. *J. Chem. Eng. Data* **1999**, *44*, 597−604.
(71) Beletskaya, I. P.; Cheprakov, A. V. The Heck Reaction as a Sharpening Stone of Palladium Catalysis. *Chem. Rev.* **2000**, *100*, 3009−3066.
(72) Mureinik, R. J.; Weitzberg, M.; Blum, J. Kinetics and Mechanism of Oxidative Addition of Aryl Iodides to Iridium(I) Complexes. *Inorg. Chem.* **1979**, *18*, 915−918.
(73) Amatore, C.; Jutand, A. Anionic Pd(0) and Pd(II) Intermediates in Palladium-Catalyzed Heck and Cross-Coupling Reactions. *Acc. Chem. Res.* **2000**, *33*, 314−321.
(74) Balcells, D.; Maseras, F.; Keay, B. A.; Ziegler, T. Polyene Cyclization by a Double Intramolecular Heck Reaction. A DFT Study. *Organometallics* **2004**, *23*, 2784−2796.
(75) Kozuch, S.; Shaik, S. A Combined Kinetic- Quantum Mechanical Model for Assessment of Catalytic Cycles: Application to Cross-Coupling and Heck Reactions. *J. Am. Chem. Soc.* **2006**, *128*, 3355−3365.
(76) Bäcktorp, C.; Norrby, P.-O. A DFT Comparison of the Neutral and Cationic Heck Pathways. *Dalton Trans.* **2011**, *40*, 11308−11314.
(77) von Schenck, H.; Åkermark, B.; Svensson, M. Electronic and Steric Ligand Effects on the Activity and Regiochemistry in the Heck Reaction. *Organometallics* **2002**, *21*, 2248−2253.
(78) Menezes da Silva, V. H.; Braga, A. A.; Cundari, T. R. N-Heterocyclic Carbene Based Nickel and Palladium Complexes: A DFT Comparison of the Mizoroki-Heck Catalytic Cycles. *Organometallics* **2016**, *35*, 3170−3181.
(79) Eremin, D. B.; Denisova, E. A.; Kostyukovich, A. Y.; Martens, J.; Berden, G.; Oomens, J.; Khrustalev, V. N.; Chernyshev, V. M.; Ananikov, V. P. Ionic Pd/NHC Catalytic System Enables Recoverable Homogeneous Catalysis: Mechanistic Study and Application in the Mizoroki-Heck Reaction. *Chem. - Eur. J.* **2019**, *25*, 16564−16572.
(80) Menezes da Silva, V. H.; Morgon, N. H.; Correia, C. R.; Braga, A. A. DFT Perspective on the Selectivity and Mechanism of Ligand-Free Heck Reaction Involving Allylic Esters and Arenediazonium Salts. *J. Organomet. Chem.* **2019**, *896*, 5−15.
(81) Surawatanawong, P.; Hall, M. B. Theoretical Study of Alternative Pathways for the Heck Reaction through Dipalladium and "ligand-Free" Palladium Intermediates. *Organometallics* **2008**, *27*, 6222−6232.
(82) Jutand, A. Mechanisms of the Mizoroki-Heck Reaction. In *The Mizoroki-Heck Reaction*; John Wiley & Sons, Ltd., 2009; pp 1−50.
(83) Kluwer, A. M.; Elsevier, C. J.; Bühl, M.; Lutz, M.; Spek, A. L. Zero-Valent Palladium Complexes with Monodentate Nitrogen σ-Donor Ligands. *Angew. Chem., Int. Ed.* **2003**, *42*, 3501−3504.
(84) Schroeter, F.; Strassner, T. Understanding Anionic "Ligandless" Palladium Species in the Mizoroki–Heck Reaction. *Inorg. Chem.* **2018**, *57*, 5159−5173.


https://dx.doi.org/10.1021/acssuschemeng.0c03523
*ACS Sustainable Chem. Eng.* 2020, 8, 9926−9936